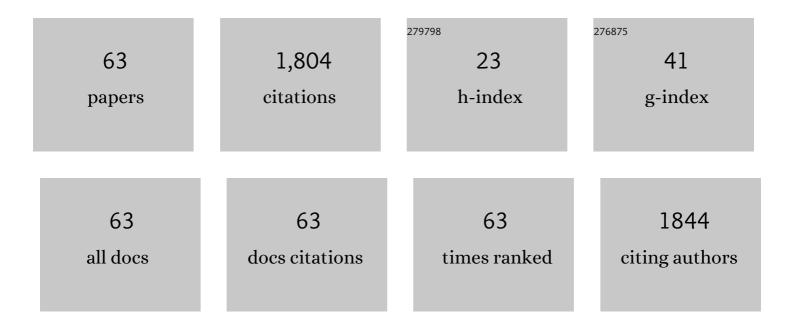
List of Publications by Year in descending order

Source: https://exaly.com/author-pdf/2904164/publications.pdf Version: 2024-02-01



CHANSHI OIN

#	Article	IF	CITATIONS
1	Local Field Modulation Induced Threeâ€Order Upconversion Enhancement: Combining Surface Plasmon Effect and Photonic Crystal Effect. Advanced Materials, 2016, 28, 2518-2525.	21.0	240
2	Passively Q-switching induced by gold nanocrystals. Applied Physics Letters, 2012, 101, .	3.3	122
3	Passively mode-locking induced by gold nanorods in erbium-doped fiber lasers. Applied Physics Letters, 2013, 103, .	3.3	119
4	Gold nanorods as saturable absorbers for all-fiber passively Q-switched erbium-doped fiber laser. Optical Materials Express, 2013, 3, 1986.	3.0	105
5	High-power mid-infrared supercontinuum laser source using fluorotellurite fiber. Optica, 2018, 5, 1264.	9.3	85
6	Greatly enhanced size-tunable ultraviolet upconversion luminescence of monodisperse β-NaYF4:Yb,Tm nanocrystals. Journal of Materials Chemistry, 2011, 21, 13413.	6.7	82
7	Enhanced deep-ultraviolet upconversion emission of Gd3+ sensitized by Yb3+ and Ho3+ in β-NaLuF4 microcrystals under 980 nm excitation. Journal of Materials Chemistry C, 2013, 1, 2485.	5.5	72
8	Holmium-doped fluorotellurite microstructured fibers for 21  μm lasing. Optics Letters, 2015, 40, 4695.	3.3	53
9	Sub-10 nm BaYF5:Yb3+,Er3+ core–shell nanoparticles with intense 1.53 μm fluorescence for polymer-based waveguide amplifiers. Journal of Materials Chemistry C, 2013, 1, 1525.	5.5	50
10	Citric acid-assisted hydrothermal synthesis of α-NaYF4:Yb3+,Tm3+ nanocrystals and their enhanced ultraviolet upconversion emissions. CrystEngComm, 2012, 14, 2302.	2.6	48
11	Passively mode-locked fiber lasers at 1039 and 1560 nm based on a common gold nanorod saturable absorber. Optical Materials Express, 2015, 5, 794.	3.0	47
12	Controlled synthesis of ultrasmall hexagonal NaTm0.02Lu0.98â^'xYbxF4 nanocrystals with enhanced upconversion luminescence. Journal of Materials Chemistry C, 2014, 2, 2037.	5.5	43
13	KMnF <sub>3</sub> :Yb <sup>3+</sup> ,Er <sup>3+</sup> @KMnF <sub>3</sub> :Yb <sup>3+</sup> active-core–active-shell nanoparticles with enhanced red up-conversion fluorescence for polymer-based waveguide amplifiers operating at 650 nm. Journal of Materials Chemistry C, 2015, 3, 9827-9832.	5.5	38
14	Synthesis of ultra-small BaLuF <sub>5</sub> :Yb <sup>3+</sup> ,Er <sup>3+</sup> @BaLuF <sub>5</sub> :Yb <sup>3+</sup> active-core–active-shell nanoparticles with enhanced up-conversion and down-conversion luminescence by a layer-by-layer strategy. Journal of Materials Chemistry C, 2015, 3, 2045-2053.	5.5	36
15	Large aspect ratio gold nanorods (LAR-GNRs) for mid-infrared pulse generation with a tunable wavelength near 3 1¼m. Optics Express, 2019, 27, 4886.	3.4	32
16	Plasmonic Cu <sub>1.8</sub> S nanocrystals as saturable absorbers for passively Q-switched erbium-doped fiber lasers. Journal of Materials Chemistry C, 2017, 5, 4034-4039.	5.5	31
17	22.7  W mid-infrared supercontinuum generation in fluorotellurite fibers. Optics Letters, 2020, 45, 1882.	3.3	30
18	Nearâ€Infrared Broadband Polymerâ€Dot Modulator with High Optical Nonlinearity for Ultrafast Pulsed Lasers. Laser and Photonics Reviews, 2019, 13, 1800326.	8.7	28

#	Article	IF	CITATIONS
19	2875 nm Lasing From Ho <sup>3+</sup> -Doped Fluoroindate Glass Fibers. IEEE Photonics Technology Letters, 2018, 30, 323-326.	2.5	27
20	Coherent supercontinuum generation from 1.4 to 4 <i>μ</i> m in a tapered fluorotellurite microstructured fiber pumped by a 1980 nm femtosecond fiber laser. Applied Physics Letters, 2017, 110, .	3.3	26
21	All-fiber-integrated Yb:YAG-derived silica fiber laser generating 6 W output power. Optics Express, 2019, 27, 3791.	3.4	26
22	Passively Mode-Locked Operations Induced by Semiconducting Polymer Nanoparticles and a Side-Polished Fiber. ACS Applied Materials & amp; Interfaces, 2020, 12, 57461-57467.	8.0	25
23	Dual mode emission of core–shell rare earth nanoparticles for fluorescence encoding. Journal of Materials Chemistry C, 2015, 3, 6314-6321.	5.5	24
24	Tunable mid-infrared Raman soliton generation from 1.96 to 2.82 μm in an all-solid fluorotellurite fiber. AIP Advances, 2018, 8, .	1.3	23
25	Mesoporous Carbon Nanospheres as Broadband Saturable Absorbers for Pulsed Laser Generation. Advanced Optical Materials, 2018, 6, 1800606.	7.3	23
26	Semiconducting polymer dots as broadband saturable absorbers for Q-switched fiber lasers. Journal of Materials Chemistry C, 2020, 8, 4919-4925.	5.5	23
27	Intense emission at â^¼3.3  µm from Er <sup>3+</sup> -doped fluoroindate glass fiber. Optics Letters, 46, 1057.	2 <u>021</u> , 3.3	22
28	Unlocking the ultrafast potential of gold nanowires for mode-locking in the mid-infrared region. Optics Letters, 2021, 46, 1562.	3.3	21
29	Gold nanowires with surface plasmon resonance as saturable absorbers for passively Q-switched fiber lasers at 2 µm. Optical Materials Express, 2019, 9, 2406.	3.0	21
30	Green/red pulsed vortex-beam oscillations in all-fiber lasers with visible-resonance gold nanorods. Nanoscale, 2019, 11, 15991-16000.	5.6	19
31	Mid-Infrared Q-Switched and Mode-Locked Fiber Lasers at 2.87 <italic>μ</italic> m Based on Carbon Nanotube. IEEE Journal of Selected Topics in Quantum Electronics, 2019, 25, 1-6.	2.9	18
32	Broadband amplification and highly efficient lasing in erbium-doped tellurite microstructured fibers. Optics Letters, 2013, 38, 1049.	3.3	17
33	Passively Q-switched erbium-doped fiber laser based on gold nanorods. Optik, 2014, 125, 5789-5793.	2.9	17
34	Efficient â^¼4  µm emission from Pr <sup>3+</sup> /Yb <sup>3+</sup> co-doped fluoroindate glass. Oµ Letters, 2021, 46, 5607.	otics 3.3	14
35	4.5 W supercontinuum generation from 1017 to 3438 nm in an all-solid fluorotellurite fiber. Applied Physics Letters, 2017, 110, 261106.	3.3	13
36	Widely tunable passively mode-locked fiber laser with carbon nanotube films. Optical Review, 2010, 17, 97-99.	2.0	12

#	Article	IF	CITATIONS
37	Tunable dual-wavelength passively mode-locked thulium-doped fiber laser using carbon nanotube. Optical Engineering, 2016, 55, 106115.	1.0	12
38	Design of a Few-Mode Erbium-Ytterbium Co-Doped Polymer Optical Waveguide Amplifier With Low Differential Modal Gain. Journal of Lightwave Technology, 2021, 39, 3201-3216.	4.6	12
39	Ceriumâ€Doped Perovskite Nanocrystals for Extremely Highâ€Performance Deepâ€Ultraviolet Photoelectric Detection. Advanced Optical Materials, 2021, 9, 2100423.	7.3	12
40	Growth of hexagonal phase sodium rare earth tetrafluorides induced by heterogeneous cubic phase core. RSC Advances, 2014, 4, 13490.	3.6	11
41	Gold nanorods saturable absorber for Q-switched Nd:GAGG lasers at 1Âμm. Applied Physics B: Lasers and Optics, 2017, 123, 1.	2.2	10
42	Mesoporous carbon nanospheres deposited onto D-shaped fibers for femtosecond pulse generation. RSC Advances, 2019, 9, 11621-11626.	3.6	10
43	25.8 W All-Fiber Mid-Infrared Supercontinuum Light Sources Based on Fluorotellurite Fibers. IEEE Photonics Technology Letters, 2022, 34, 367-370.	2.5	10
44	Broadband supercontinuum generation from 600 to 5400 nm in a tapered fluorotellurite fiber pumped by a 2010 nm femtosecond fiber laser. Applied Physics Letters, 2019, 115, 091103.	3.3	9
45	KMnF3:Yb3+,Er3+ Core-Active-Shell Nanoparticles with Broadband Down-Shifting Luminescence at 1.5 μm for Polymer-Based Waveguide Amplifiers. Nanomaterials, 2019, 9, 463.	4.1	9
46	2.074- Lasing From Ho <sup>3+</sup> -Doped Fluorotellurite Microstructured Fibers Pumped by a 1120-nm Laser. IEEE Photonics Technology Letters, 2016, 28, 1084-1087.	2.5	8
47	Wideband Tunable, Carbon Nanotube Mode-Locked Fiber Laser Emitting at Wavelengths Around \$3~mu\$ m. IEEE Photonics Technology Letters, 2019, 31, 869-872.	2.5	8
48	Single-Frequency kHz-Linewidth 1070 nm Laser Based on Yb:YAG Derived Silica Fiber. IEEE Photonics Technology Letters, 2020, 32, 895-898.	2.5	8
49	Design of Fluorotellurite Microstructured Fibers With Near-Zero-Flattened Dispersion Profiles for Optical-Frequency Comb Generation. Journal of Lightwave Technology, 2018, 36, 2211-2215.	4.6	7
50	MnO <sub>2</sub> nanosheets as saturable absorbers for a Q-switched fiber laser. Optical Materials Express, 2020, 10, 3097.	3.0	7
51	Sapphire-Derived Fiber Bragg Gratings for High Temperature Sensing. Crystals, 2021, 11, 946.	2.2	6
52	Silver Nanowires with Ultrabroadband Plasmon Response for Ultrashort Pulse Fiber Lasers. Advanced Photonics Research, 2022, 3, .	3.6	6
53	Ho <sup>3+</sup> /Pr <sup>3+</sup> Co-Doped AlF <sub>3</sub> Based Glass Fibers for Efficient ~2.9 <i>îl¼</i> m Lasers. IEEE Photonics Technology Letters, 2020, 32, 1489-1492.	2.5	6
54	Linearly polarized single-frequency fiber laser based on the Yb:YAG-crystal derived silica fiber. Applied Optics, 2020, 59, 9931.	1.8	5

#	Article	IF	CITATIONS
55	Stable Dissipative Soliton Generation From Yb-Doped Fiber Laser Modulated via Evanescent Field Interaction With Gold Nanorods. IEEE Photonics Journal, 2018, 10, 1-8.	2.0	4
56	Q-switched lasing at the 2 µm wavelength induced by Cu <sub>18</sub> S nanocrystals. OSA Continuum, 2019, 2, 2809.	1.8	4
57	Triangular gold nanoplates as saturable absorber for passively Q-switched fiber laser at 1.56 μm. Laser Physics Letters, 2021, 18, 095101.	1.4	3
58	Cascaded Raman amplifiers based on fluorotellurite fibers. Optical Materials Express, 2022, 12, 2309.	3.0	2
59	Flying upconversion fluorescent particles and direct observation of energy transfer and depopulation processes. CrystEngComm, 2015, 17, 587-591.	2.6	1
60	Enhancement of phase-matched third harmonic generation via soliton self-frequency shift cancellation in a fluorotellurite microstructured fiber. Applied Physics Letters, 2017, 111, 151103.	3.3	1
61	Amplification of wavelength-shifting soliton in active photonic crystal fibers. Applied Physics Letters, 2018, 112, 161105.	3.3	1
62	Dual-wavelength mode-locked thulium-doped fiber laser based on carbon nanotube. , 2016, , .		0
63	Fluorotellurite Microstructured Fibers and Their Applications. , 2018, , .		0